GEOLOGY | THE GEOLOGICAL SOCIETY OF AMERICA®

https://doi.org/10.1130/G49286.1

Manuscript received 12 November 2020
Revised manuscript received 4 August 2021
Manuscript accepted 11 August 2021

Published online 20 October 2021

Formation of low-gradient bedrock chutes by dry rockfall on planetary surfaces

Zhongheng Sun[1,2], Thomas P. Ulizio[1], Jade N. Fischer[1], Janette N. Levin[1], Alexander R. Beer[1,3], James L. Dickson[1] and Michael P. Lamb[1]*

[1]Division of Geological and Planetary Sciences, California Institute of Technology, Pasadena, California 91125, USA
[2]Key Laboratory of Tectonics and Petroleum Resources (China University of Geosciences), Ministry of Education, Wuhan 430074, China
[3]Department of Geosciences, University of Tübingen, D-72076 Tübingen, Germany

ABSTRACT

Channel-like forms are ubiquitous on steep hillslopes on Earth, Mars, and other planetary bodies. On Earth and Mars, these landforms are commonly attributed to water activity, especially for slopes below the angle of repose (~30°) where dry granular flows are considered ineffective. While the angle of repose characterizes loose sediment stability, it is unclear whether dry rockfall can traverse and erode channels in bedrock or cemented substrates. We used a large-scale experiment to show that bedrock chutes can form spontaneously at low gradients from dry rockfall. Our results, combined with observations of rocky outcrops and boulders on Mars, indicate that rockfall can be an important bedrock degradation process that can produce low-gradient channels in the absence of water.

INTRODUCTION

Steep channel-like landforms—referred to as bedrock chutes—are ubiquitous landforms on a wide range of hillslopes on Earth, Mars (Dickson and Head, 2009), the Moon (Kumar et al., 2013), and other planetary bodies (Krohn et al., 2014). On Mars, bedrock chutes are particularly important because they line the rocky walls of craters at all latitudes and may indicate volatile activity (Dickson and Head, 2009) (Fig. 1A; Fig. S1 in the Supplemental Material[1]). Bedrock chutes are different than, but sometimes related to, martian gullies. Gullies consist of an incised alcove, a main channel, and a fan downslope (Fig. S1B), resembling water-worn landforms on Earth (Malin and Edgett, 2000). Coalescing bedrock chutes commonly compose the channelized skeleton of gully alcoves, and in many cases, especially at low latitudes, chutes exist in the absence of well-incised gullies (Dickson and Head, 2009). The latitude-dependent distribution and orientation preference of gully channels (Heldmann and Mellon, 2004; Dickson et al., 2007; Harrison et al., 2015) have been used as evidence for liquid water (Malin and Edgett, 2000), brines (Heldmann and Mellon, 2004), or water ice–driven processes (Williams et al., 2009). However, it is not known whether bedrock chutes also require volatiles to form.

Given the relative youth of gullies (Malin and Edgett, 2000), a primary criticism of the "wet hypothesis" for gully formation is that water is not stable on the martian surface today (Musselwhite et al., 2001; Treiman, 2003). Alternate models considered gully and chute formation by dry granular flow or rockfall in the absence of water (Treiman, 2003; Shinbrot et al., 2004; Kumar et al., 2013). The dry hypothesis has been challenged primarily because some landforms occur considerably below the angle of repose of loose sediment (30°–40°; Fig. 1) (Heldmann and Mellon, 2004; Dickson et al., 2007; Conway et al., 2015). For terrestrial bedrock chutes, it is difficult to separate dry and wet processes. Nonetheless, terrestrial dry granular flows over loose sediment substrates do not carve channels and instead form lobes or conical slopes near the angle of repose (Selby, 1982). The same phenomenon has been observed on the lee slope of aeolian dunes on Mars (Fig. S1E), where grain flows rest at a similar angle as on Earth (~30°) (Atwood-Stone and McEwen, 2013).

While numerical models can produce dry granular flows that run out to lower gradients if small dynamic friction angles are imposed (Pelletier et al., 2008), the reason for reduced friction is unclear. One possibility on Mars is that outbursts of CO_2 gas destabilize loose sediment (Hoffman, 2002; Dundas et al., 2019a) and lubricate dry avalanches, exposing an ice-cemented sediment substrate to sublimation, which deepens the channel (Pilorget and Forget, 2016; Sylvest et al., 2016). We explored an additional possibility for formation of channelized landforms whereby dry rockfall erodes an indurated substrate—either bedrock or ice-cemented or otherwise cohesive colluvium—through wear due to repetitive impacts. In contrast to granular flows over a loose bed of sediment, rockfall might traverse low slopes on a strong substrate because of large particle sizes relative to the substrate roughness height (DiBiase et al., 2017), which reduces friction (Fig. 2).

METHODS

We conducted an experiment using a 2.2-m-long, 0.755-m-wide test section with an initially planar bed of synthetic bedrock tilted to 16.7°, and subjected it to repeated rockfall that traversed the test section. The experiment (Fig. S2) had a floor composed of polyurethane foam of low tensile strength (0.32 MPa), which was used previously as a bedrock analog and follows the same tensile strength–erosion scaling law as natural rock (Scheingross et al., 2014). The flume slope was near the lower range observed for martian gullies (Fig. 1) and far lower than the friction angle of the sediment resting on a bed of similar-sized sediment (34°; Fig. 2; Fig. S3C). Nonetheless, the rockfall was able to

*E-mail: mpl@caltech.edu

[1]Supplemental Material. Supplemental Figures S1–S8, Videos S1–S3, and Data files S1–S8. Please visit https://doi.org/10.1130/GEOL.S.16746229 to access the supplemental material, and contact editing@geosociety.org with any questions.

CITATION: Sun, Z., et al., 2021, Formation of low-gradient bedrock chutes by dry rockfall on planetary surfaces: Geology, v. XX, p. , https://doi.org/10.1130/G49286.1

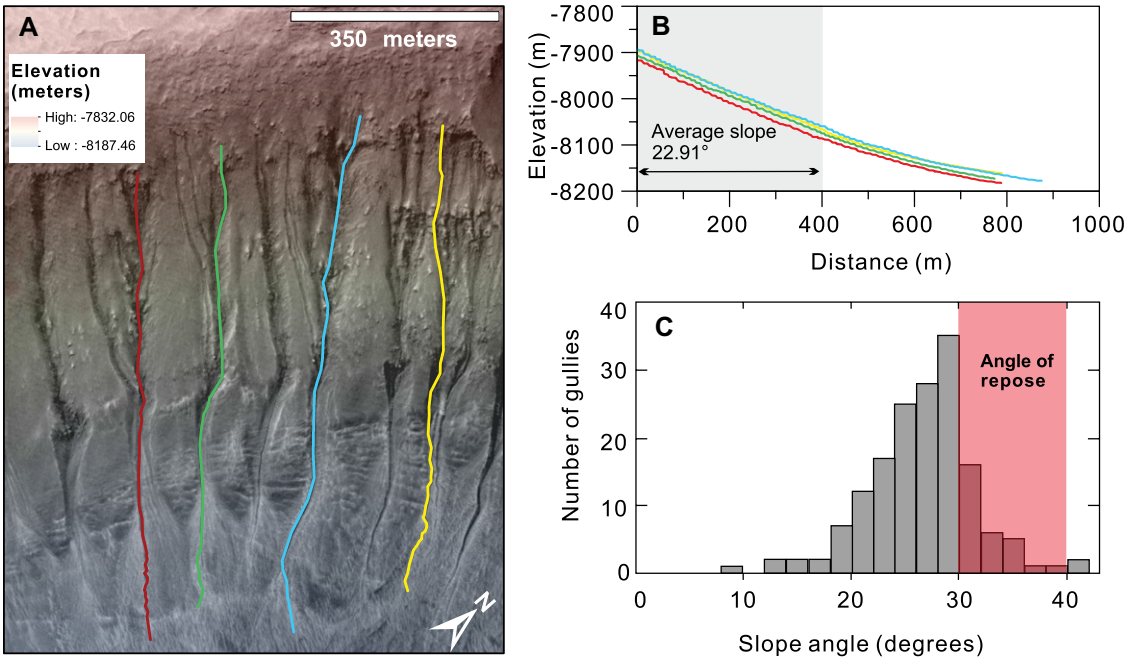

Figure 1. Low-gradient gullies on Mars. (A) Mars Reconnaissance Orbiter High Resolution Imaging Science Experiment (HiRISE) image PSP_004176_1405 (latitude [centered]: –39.359°, longitude (east): 202.664°); topography generated from HiRISE digital elevation model constructed with Ames Stereo Pipeline software (https://ti.arc.nasa.gov/tech/asr/groups/intelligent-robotics/ngt/stereo/) using images PSP_004176_1405 and PSP_005587_1405. (B) Elevation profiles from panel A. (C) Frequency distribution of martian gullies averaged over gully length in 2° bins measured from Mars Orbiter Laser Altimeter (MOLA) data (Dickson et al., 2007). Image credits: NASA/JPL-Caltech/University of Arizona.

transverse the bedrock slope because particle friction angles on the foam (median 20°; Fig. 2; Fig. S3C) were lower owing to large particle diameters, D, relative to the foam roughness height, σ (DiBiase et al., 2017).

We used natural fluvial cobbles (D_{16} [diameter at which 16% of pebbles are smaller] = 53.64 mm, D_{50} = 61 mm, and D_{84} = 69 mm; Fig. S3A; Data file S1). The particles were round to achieve the low friction angles expected for much larger natural angular rockfall (Fig. 2). Friction angles, ϕ_f, of 28 particles from the experiment were measured using tilt tables following the method of Prancevic and Lamb (2015) for both an uneroded foam bed ($\phi_f = 20°$) and a bed of fixed particles of like size ($\phi_f = 34°$) (Fig. S3C; Data file S2). The roughness height for each of the substrates (0.18 mm for foam, 17.06 mm for the fixed particle bed) was determined using a sub-millimeter-accuracy topographic scan, subtracting a fitted plane, and taking the root mean square of the residuals. Particles were recirculated using a series of conveyor belts at a constant rate and introduced sparsely (with minimal particle-particle interactions) into the flume from a 0.5 m drop onto an inclined ramp (Fig. S2).

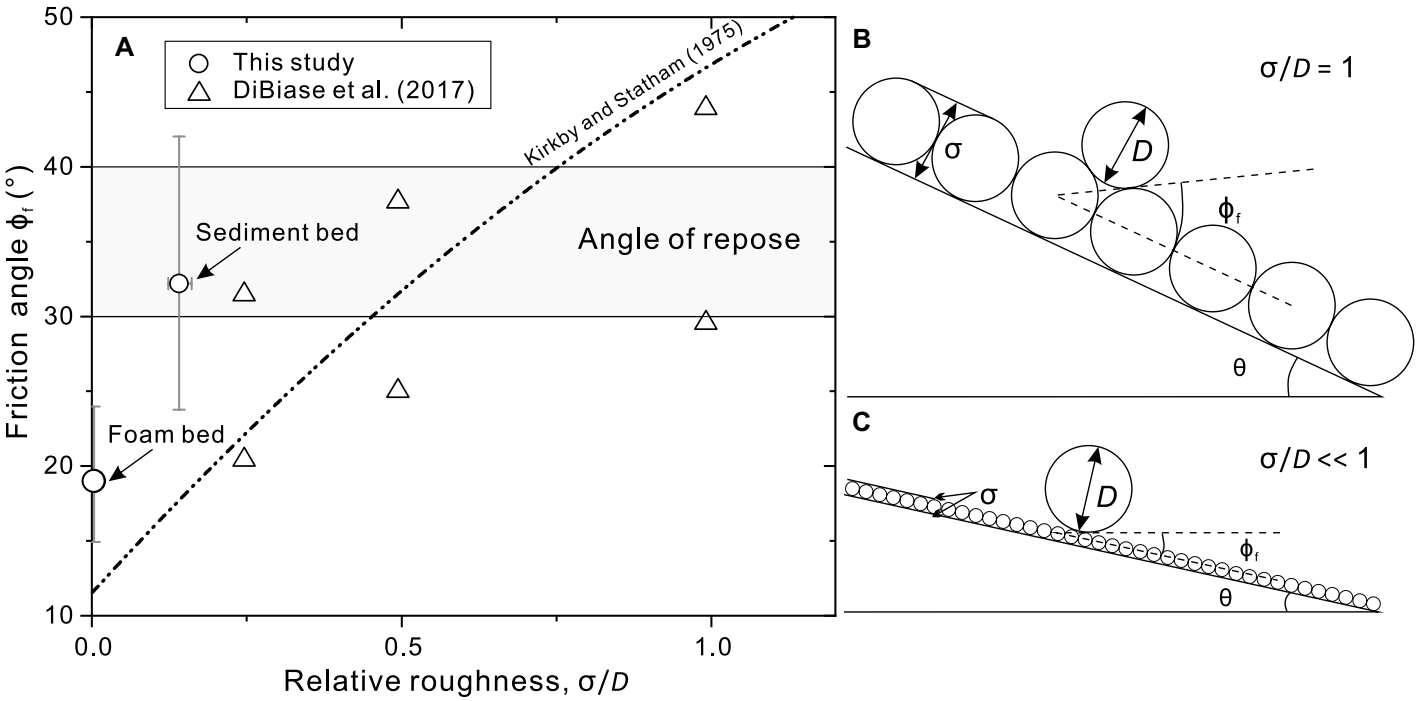

Figure 2. (A) Static friction angle, ϕ_f, versus relative roughness (roughness height, σ, normalized by particle diameter, D) for our study (see Data file S2 [see footnote 1]) and prior work (Kirkby and Statham, 1975; DiBiase et al., 2017). Circles are geometric mean; error bars are geometric standard deviation. Typical angle of repose for natural sand and gravel is demarked as 30°–40°. (B,C) Particle at incipient failure (i.e., hillslope gradient $\theta = \phi_f$) for cases of large ($\sigma/D = 1$) (B) and small ($\sigma/D << 1$) (C) relative roughness.

We used particle imaging velocimetry (PIV) to measure particle trajectories from side-view images (60 frames per second [fps]) using Python-based software packages (OpenCV and TrackPy; https://github.com/opencv/opencv-python, http://soft-matter.github.io/trackpy/v0.5.0/) (Fig. S2A). From these trajectories, we calculated particle hop height, Δh, as the maximum trajectory height normal to the bed, and particle hop length, Δl, as the along-slope distance between consecutive bed impacts (Fig. S4; Data file S3). We calculated bed-normal impact velocity, $v_{in,y}$, and particle impact energy ($\frac{1}{2}m_g v_{in,y}^2$), where $m_g = 341$ g is the median particle mass (Fig. S3B). We used plan-view images (from PIV cameras 4–6; Fig. S2A) to calculate the cross-slope distribution of particles by finding the intersection between the particle trajectory and a defined cross-section transect for ~700 particles (Data file S4). These distributions did not change substantially in shape when using >~500 particles (Fig. S5; Data file S5).

Bedrock topography was measured every 40–60 min using an automated cart system with a laser distance meter of 1 mm along-slope spacing, 5 mm cross-slope spacing, and a vertical resolution of ~0.1 mm. Scans were analyzed using the CloudCompare (version 2.11; http://www.cloudcompare.org/) M3C2 plugin to compute vertical differences between consecutive point clouds and the initial surface (Fig. S6; Lague et al., 2013). Results are presented using a dimensionless experimental time:

$$T^* = \frac{1}{m_g}\int_0^t Q_s dt, \quad (1)$$

in which t is experiment time and Q_s is the mass discharge of sediment. T^* normalizes slight variations in sediment supply and is equivalent to the cumulative number of particles that traversed the test section (Fig. S7; Data file S6). The normalized instantaneous erosion rate was calculated as:

$$E_i = -\overline{(z_i - z_{i-1})}\,/(T_i^* - T_{i-1}^*), \quad (2)$$

in which $\overline{(z_i - z_{i-1})}$ is the point-by-point elevation change between the scan at time i and the previous scan, averaged over the test section (Data files S7 and S8).

RESULTS

Within the first 3 h ($T^* < 24{,}800$) of the experiment, particles slowly and uniformly abraded the initially planar bedrock surface (Fig. 3B). Particles moved through the test section by repetitive hopping (Videos S1–S3) with median hop heights of 0.021 m, hop lengths of 0.12 m, bed-normal impact velocities of 0.12 m/s, and downslope velocities of 1.0 m/s (Fig. S4), and erosion occurred due to grain impacts (e.g., Beer and Lamb, 2021). After $T^* = 24{,}800$, spatially variable erosion rates led to the formation of downslope repeating bedrock depressions and steps (Fig. 3B; Fig. S6), similar to cyclic steps formed in previous experiments on riverbed incision that used flowing water and bedload (Scheingross et al., 2019). High-speed cameras revealed a particle hop length similar to step wavelength (Fig. 3B). Particles impacted on the upslope side of the depressions (Fig. 3C), causing the steps to migrate downslope (Fig. 3B). Erosion was generally greater in the center of the depressions, and by $T^* = 57{,}100$, several depressions began to coalesce to form a single, alcove-like depression and a channel-like trough further downslope (Fig. 3A; Fig. S6; Video S1). By $T^* = 66{,}100$, the depression exceeded 0.12 m in depth and began to hold a permanent cover of sediment that prevented it from further erosion (Fig. S8C); subsequent incoming particles traversed the cover and continued to erode the channel downslope.

Dry rockfall in our experiment channelized the bedrock slope due to a feedback between the evolving topography, sediment transport, and bedrock erosion. Early in the experiment, the cross-slope distribution of particles was uniform in the center of the flume ($T^* = 0$ in Figs. 4D–4F) owing to the tilted peg board upstream of the test section used to disperse the particles (Fig. S2); however, unintentional gaps in pegs near the flume walls (Fig. S8A) led to a greater number of particles transported

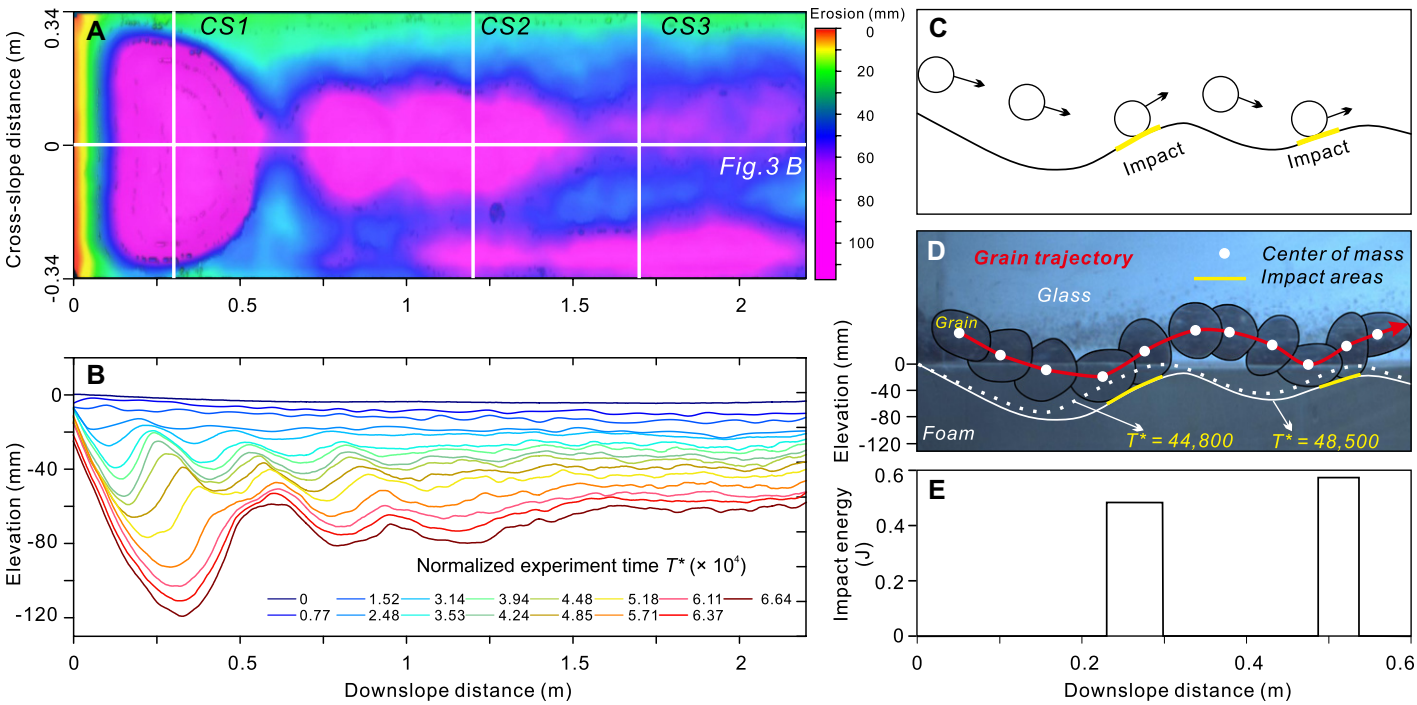

Figure 3. Channelization in flume experiment. (A) Measured total vertical erosion. Locations of cross sections CS1–CS3 (Fig. 4) are shown. (B) Topographic scans showing centerline profile evolution (see Data file S8 [see footnote 1]). T^*—dimensionless experimental time. (C) Schematic diagram of trough formation process. (D) Grains impacting on trough recorded by side-view camera. (E) Calculated impact energy of grains along flume.

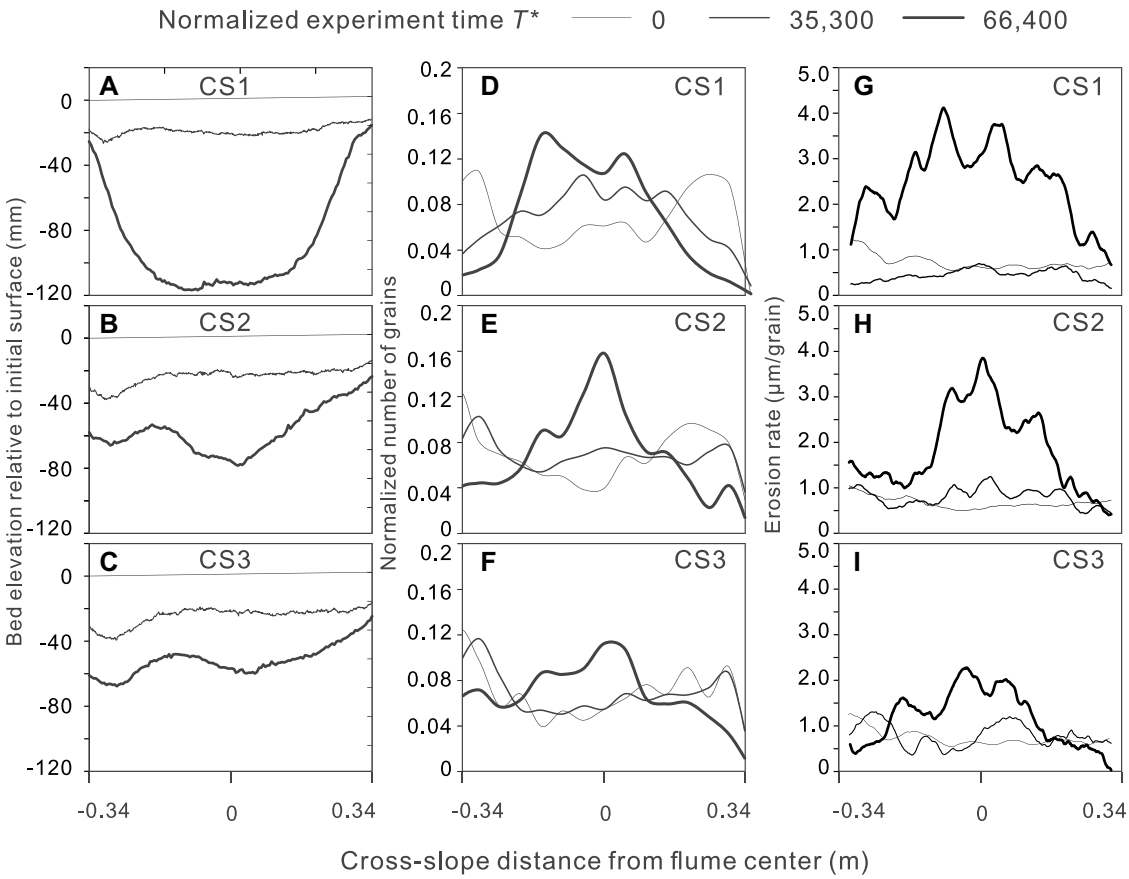

Figure 4. Experiment cross sections at locations CS1–CS3 on Figure 3A (downslope positions of 0.325, 1.225 and 1.725 m, respectively) at three different times (*T—dimensionless experimental time). (A–C) Bed topography. (D–F) Number of particles that crossed CS1–CS3 binned in 5 cm intervals across slope, normalized by sum of all transited grains during that interval (see Data file S4 [see footnote 1]). (G–I) Normalized erosion rate (Equation 2) smoothed with median sliding window of 0.05 m width (Data file S7).**

along the walls. Consequently, we removed all pegs from the board except near the edges (Fig. S8B) early in the experiment, which produced a more Gaussian cross-slope distribution of particles entering the test section after $T^* = 7700$ (e.g., see $T^* = 35{,}300$ in Fig. 4D). Nonetheless, the bedrock channel that developed along the right sidewall (cross-slope distance of −0.3 m; Fig. 3A) during $T^* < 7700$ continued to focus particles into it (Figs. 4D–4F), resulting in enhanced erosion and channelization there that persisted throughout the experiment (Fig. 4H). Likewise, after the adjustment of the inlet particle distribution to favor the flume center, enhanced erosion rates in the middle of the test section (Figs. 4G–4I) further deepened the channel there (Figs. 4A–4C; Fig. S6). By the end of the experiment at $T^* = 66{,}400$, the cross-slope distributions of particles (Figs. 4D–4F) and the erosion rate (Figs. 4G–4I) were substantially more weighted to the center of the flume as compared to earlier in the experiment, illustrating topographic steering of grain trajectories that focused erosion and caused channelization (Fig. S8). Channelization and particle focusing was likely enhanced as the chute relief became comparable to particle hop height (~21 mm) midway through the experiment.

The experiment ended because the upslope depression had deepened and widened to the point that the local particle cover spanned the entire width of the test section, which blocked transport (Fig. S8C). This condition corresponded to cross-sectional relief of the upslope depression of 120 mm, which is notably greater than one particle diameter and therefore the depth in which static particles were sheltered from mobilization by collisions. While the sediment pile created a barrier in our experiment, natural chutes do not have limiting sidewalls. Instead, we expect natural rockfall would have either been deflected around the rough patch or the pile would have steepened past the angle of repose, resulting in avalanching. Small bedrock irregularities can create focal points for erosion, corralling moving sediment into topographic lows, as happened along the sidewall in our experiment. Natural chutes often source rockfall from steep cliffs, and momentum from this vertical drop can aid transport, as compared to our experiments where inlet particle velocities were limited to ~1 m/s (Fig. S4D).

DISCUSSION AND CONCLUSIONS

Our experiment illustrated that low-gradient bedrock chutes can form by dry rockfall erosion even at slopes well below the angle of repose. We expect that channelization due to progressive wear by repetitive impacts should occur for more concentrated dry granular flows or rock avalanches (Farin et al., 2019) in addition to the sparse rockfall in our experiment. The channelization mechanism likely can occur at any topographic gradient where particles can move under the influence of gravity, including slopes above and below the angle of repose.

In comparison to granular flows over loose sediment (Selby, 1982), our results showed that an erodible material with strength is the key to allowing dry rockfall channelization. Unlike dry grains traversing a slope of loose particles, the friction angle for sediment traversing an indurated substrate can be far smaller than the angle of repose—as it was in our experiment—if the grain size in transport, D, is large relative to the characteristic roughness height of the substrate, σ (Fig. 2) (DiBiase et al., 2017). Moreover, cohesive substrates can hold their form over time, allowing for persistent topographic steering of particle paths and morphodynamic feedback.

Martian craters commonly have a rocky rim with steep cliffs and promontories that surround bedrock chutes (Fig. 1; Fig. S1). These areas are likely sources of rockfall (Figs. S1C and S1D) that could be triggered by ice or frost (Pilorget and Forget, 2016; Sylvest et al., 2016), solar-induced thermal stress, marsquakes, meteor impacts, wind, or rock fatigue (Roberts et al., 2012; Tesson et al., 2020). Boulder tracks on crater walls show that rockfall is an active process on Mars (Dundas et al., 2019b; Tesson et al., 2020) and the Moon (Bickel et al., 2019). For instance, if the roughness height is $\sigma < 0.3$ m, 2 m diameter boulders should be effective in chute formation at hillslope gradients of 20° or

less (Fig. 2). Rockfall erosion might be particularly important for martian equatorial gullies, many of which are weakly incised straight chutes that can occur in weak sulfate rocks (Auld and Dixon, 2016; Thomas et al., 2020).

In some cases, bedrock chutes on Mars coalesce into larger alcoves in association with gullies (Fig. S1A) (Malin and Edgett, 2000). Our results suggest that, in addition to producing bedrock chutes and alcoves, dry rockfall might be an important contributor in incising gully channels into ice-rich mantling material (Christensen, 2003) or other cohesive sediment substrates that have strength. Therefore, along with sublimation and dry avalanching (Pilorget and Forget, 2016; Tesson et al., 2020), gully incision might occur from rockfall impacts that mechanically wear the channel floor. Runout might be further aided by CO_2 frost or gas lubricating the granular flows (Hugenholtz, 2008; Pilorget and Forget, 2016), although our experiment indicates that lubricating agents are necessary for large particle sizes on relatively smooth, indurated substrates. We do not expect that reduced gravity on Mars substantially impacts rockfall channelization; however, with all else equal (e.g., initial drop height, rockfall size, bedrock strength), impact energies, and therefore erosion rates, should be lower with reduced gravity (Beer and Lamb, 2021).

Our results suggest that dry rockfall could be an important process in degrading rocky or indurated hillslopes on Mars (Conway et al., 2015), the Moon (Kumar et al., 2013), and the asteroid Vesta (Krohn et al., 2014), potentially even at relatively low gradients. While well-incised martian gullies have been linked to volatile activity, our work indicates that impact wear from dry rockfall might also contribute to aspects of gully formation in addition to bedrock chutes. Nonetheless, quantitatively diagnosing wet or dry processes from steep channelized landforms remains a challenge, especially on Earth where the impact of water is ubiquitous.

ACKNOWLEDGMENTS

Funding was provided by NASA grant 80NSSC19K1269 to M.P. Lamb. Z. Sun was supported by China Scholarship Council grant 201906410043 and H. Zhu, and A.R. Beer by Swiss National Science Foundation grant P2EZP2_172109. We thank Tim Goudge, Colin Dundas, Susan Conway, and anonymous reviewers for helpful comments.

REFERENCES CITED

Atwood-Stone, C., and McEwen, A.S., 2013, Avalanche slope angles in low-gravity environments from active Martian sand dunes: Geophysical Research Letters, v. 40, p. 2929–2934, https://doi.org/10.1002/grl.50586.

Auld, K.S., and Dixon, J.C., 2016, A classification of Martian gullies from HiRISE imagery: Planetary and Space Science, v. 131, p. 88–101, https://doi.org/10.1016/j.pss.2016.08.002.

Beer, A.R., and Lamb, M.P., 2021, Abrasion regimes in fluvial bedrock incision: Geology, v. 49, p. 682–686, https://doi.org/10.1130/G48466.1.

Bickel, V.T., et al., 2019, Analysis of lunar boulder tracks: Implications for trafficability of pyroclastic deposits: Journal of Geophysical Research: Planets, v. 124, p. 1296–1314, https://doi.org/10.1029/2018JE005876.

Christensen, P.R., 2003, Formation of recent martian gullies through melting of extensive water-rich snow deposits: Nature, v. 422, p. 45–48, https://doi.org/10.1038/nature01436.

Conway, S.J., Balme, M.R., Kreslavsky, M.A., Murray, J.B., and Towner, M.C., 2015, The comparison of topographic long profiles of gullies on Earth to gullies on Mars: A signal of water on Mars: Icarus, v. 253, p. 189–204, https://doi.org/10.1016/j.icarus.2015.03.009.

DiBiase, R.A., Lamb, M.P., Ganti, V., and Booth, A.M., 2017, Slope, grain size, and roughness controls on dry sediment transport and storage on steep hillslopes: Journal of Geophysical Research: Earth Surface, v. 122, p. 941–960, https://doi.org/10.1002/2016JF003970.

Dickson, J.L., and Head, J.W., 2009, The formation and evolution of youthful gullies on Mars: Gullies as the late-stage phase of Mars' most recent ice age: Icarus, v. 204, p. 63–86, https://doi.org/10.1016/j.icarus.2009.06.018.

Dickson, J.L., Head, J.W., and Kreslavsky, M., 2007, Martian gullies in the southern mid-latitudes of Mars: Evidence for climate-controlled formation of young fluvial features based upon local and global topography: Icarus, v. 188, p. 315–323, https://doi.org/10.1016/j.icarus.2006.11.020.

Dundas, C.M., McEwen, A.S., Diniega, S., Hansen, C.J., Byrne, S., and McElwaine, J.N., 2019a, The formation of gullies on Mars today, *in* Conway, S.J., et al., eds., Martian Gullies and their Earth Analogues: Geological Society [London] Special Publication 467, p. 67–94, https://doi.org/10.1144/SP467.5.

Dundas, C.M., Mellon, M.T., Conway, S.J., and Gastineau, R., 2019b, Active boulder movement at high Martian latitudes: Geophysical Research Letters, v. 46, p. 5075–5082, https://doi.org/10.1029/2019GL082293.

Farin, M., Tsai, V.C., Lamb, M.P., and Allstadt, K.E., 2019, A physical model of the high-frequency seismic signal generated by debris flows: Earth Surface Processes and Landforms, v. 44, p. 2529–2543, https://doi.org/10.1002/esp.4677.

Harrison, T.N., Osinski, G.R., Tornabene, L.L., and Jones, E., 2015, Global documentation of gullies with the Mars Reconnaissance Orbiter Context Camera and implications for their formation: Icarus, v. 252, p. 236–254, https://doi.org/10.1016/j.icarus.2015.01.022.

Heldmann, J.L., and Mellon, M.T., 2004, Observations of martian gullies and constraints on potential formation mechanisms: Icarus, v. 168, p. 285–304, https://doi.org/10.1016/j.icarus.2003.11.024.

Hoffman, N., 2002, Active polar gullies on Mars and the role of carbon dioxide: Astrobiology, v. 2, p. 313–323, https://doi.org/10.1089/153110702762027899.

Hugenholtz, C.H., 2008, Frosted granular flow: A new hypothesis for mass wasting in martian gullies: Icarus, v. 197, p. 65–72, https://doi.org/10.1016/j.icarus.2008.04.010.

Kirkby, M.J., and Statham, I., 1975, Surface stone movement and scree formation: The Journal of Geology, v. 83, p. 349–362, https://doi.org/10.1086/628097.

Krohn, K., et al., 2014, Mass movement on Vesta at steep scarps and crater rims: Icarus, v. 244, p. 120–132, https://doi.org/10.1016/j.icarus.2014.03.013.

Kumar, P.S., Keerthi, V., Kumar, A.S., Mustard, J., Krishna, B.G., Amitabh, Ostrach, L.R., Kring, D.A., Kumar, A.S.K., and Goswami, J.N., 2013, Gullies and landslides on the Moon: Evidence for dry-granular flows: Journal of Geophysical Research: Planets, v. 118, p. 206–223, https://doi.org/10.1002/jgre.20043.

Malin, M.C., and Edgett, K.S., 2000, Evidence for recent groundwater seepage and surface runoff on Mars: Science, v. 288, p. 2330–2335, https://doi.org/10.1126/science.288.5475.2330.

Musselwhite, D.S., Swindle, T.D., and Lunine, J.I., 2001, Liquid CO_2 breakout and the formation of recent small gullies on Mars: Geophysical Research Letters, v. 28, p. 1283–1285, https://doi.org/10.1029/2000GL012496.

Pelletier, J.D., Kolb, K.J., McEwen, A.S., and Kirk, R.L., 2008, Recent bright gully deposits on Mars: Wet or dry flow?: Geology, v. 36, p. 211–214, https://doi.org/10.1130/G24346A.1.

Pilorget, C., and Forget, F., 2016, Formation of gullies on Mars by debris flows triggered by CO_2 sublimation: Nature Geoscience, v. 9, p. 65–69, https://doi.org/10.1038/ngeo2619.

Prancevic, J.P., and Lamb, M.P., 2015, Particle friction angles in steep mountain channels: Journal of Geophysical Research: Earth Surface, v. 120, p. 242–259, https://doi.org/10.1002/2014JF003286.

Roberts, G.P., Matthews, B., Bristow, C., Guerrieri, L., and Vetterlein, J., 2012, Possible evidence of paleomarsquakes from fallen boulder populations, Cerberus Fossae, Mars: Journal of Geophysical Research, v. 117, E02009, https://doi.org/10.1029/2011JE003816.

Scheingross, J.S., Brun, F., Lo, D.Y., Omerdin, K., and Lamb, M.P., 2014, Experimental evidence for fluvial bedrock incision by suspended and bedload sediment: Geology, v. 42, p. 523–526, https://doi.org/10.1130/G35432.1.

Scheingross, J.S., Lamb, M.P., and Fuller, B.M., 2019, Self-formed bedrock waterfalls: Nature, v. 567, p. 229–233, https://doi.org/10.1038/s41586-019-0991-z.

Selby, M.J., 1982, Hillslope Materials and Processes: Oxford, UK, Oxford University Press, 264 p.

Shinbrot, T., Duong, N.-H., Kwan, L., and Alvarez, M.M., 2004, Dry granular flows can generate surface features resembling those seen in Martian gullies: Proceedings of the National Academy of Sciences of the United States of America, v. 101, p. 8542–8546, https://doi.org/10.1073/pnas.0308251101.

Sylvest, M.E., Conway, S.J., Patel, M.R., Dixon, J.C., and Barnes, A., 2016, Mass wasting triggered by seasonal CO_2 sublimation under Martian atmospheric conditions: Laboratory experiments: Geophysical Research Letters, v. 43, p. 12,363–12,370, https://doi.org/10.1002/2016GL071022.

Tesson, P.A., Conway, S.J., Mangold, N., Ciazela, J., Lewis, S.R., and Mège, D., 2020, Evidence for thermal-stress-induced rockfalls on Mars impact crater slopes: Icarus, v. 342, 113503, https://doi.org/10.1016/j.icarus.2019.113503.

Thomas, M.F., McEwen, A.S., and Dundas, C.M., 2020, Present-day mass wasting in sulfate-rich sediments in the equatorial regions of Mars: Icarus, v. 342, 113566, https://doi.org/10.1016/j.icarus.2019.113566.

Treiman, A.H., 2003, Geologic settings of Martian gullies: Implications for their origins: Journal of Geophysical Research, v. 108, 8031, https://doi.org/10.1029/2002JE001900.

Williams, K.E., Toon, O.B., Heldmann, J.L., and Mellon, M.T., 2009, Ancient melting of mid-latitude snowpacks on Mars as a water source for gullies: Icarus, v. 200, p. 418–425, https://doi.org/10.1016/j.icarus.2008.12.013.

Printed in USA